Journal of Neural Engineering

Rapidly formed stable and aligned dense collagen gels seeded with Schwann cells support peripheral nerve regeneration

To cite this article before publication: Papon Muangsanit *et al* 2020 *J. Neural Eng.* in press https://doi.org/10.1088/1741-2552/abaa9c

Rapidly Formed Stable and Aligned Dense Collagen Gels Seeded with Schwann Cells Support Peripheral Nerve Regeneration

Papon Muangsanit[1,2,4,*], Adam Day[1,2,4], Savvas Dimiou[4], Altay Frederick Ataç[4], Céline Kayal[2,4,5], Hyeree Park[3], Showan N Nazhat[3], James Phillips[1,2,4]

[1]*Department of Biomaterials and Tissue Engineering, Eastman Dental Institute, University College London, 256 Grays Inn Rd, London WC1X 8LD, United Kingdom*

[2]*UCL Centre for Nerve Engineering, University College London, London, United Kingdom*

[3]*Department of Mining and Materials Engineering, McGill University, 3610 Rue University, Montréal, QC H3A 0C5, Canada*

[4]*Department of Pharmacology, UCL School of Pharmacy, University College London, 29-39 Brunswick Square, Bloomsbury, London WC1N 1AX, United Kingdom*

[5]*Department of Mechanical Engineering, Roberts Engineering Building, University College London, Torrington Place, London WC1E 7JE, United Kingdom*

**Corresponding Author.*
Papon Muangsanit
Department of Pharmacology, UCL School of Pharmacy, University College London, 29-39 Brunswick Square, Bloomsbury, London WC1N 1AX, United Kingdom
Email: papon.muangsanit.14@ucl.ac.uk

Abstract

Objective. Gel aspiration-ejection (GAE) has recently been developed for the rapid production of dense, anisotropic collagen gel scaffolds with adjustable collagen fibrillar densities. In this study, a GAE system was applied to produce aligned Schwann cells within a type-1 collagen matrix to generate GAE-engineered neural tissues (GAE-EngNT) for potential nerve tissue engineering applications. *Approach.* The stability and mechanical properties of the constructs were investigated along with the viability, morphology and distribution of Schwann cells. Having established the methodology to construct stable robust Schwann cell-loaded engineered neural tissues using GAE (GAE-EngNTs), the potential of these constructs in supporting and guiding neuronal regeneration, was assessed both *in vitro* and *in vivo*. *Main results.* Dynamic mechanical analysis strain and frequency sweeps revealed that the GAE-EngNT produced via cannula gauge number 16G (~1.2 mm diameter) exhibited similar linear viscoelastic behaviors to rat sciatic nerves. The viability and alignment of seeded Schwann cell in GAE-EngNT were maintained over time post GAE, supporting and guiding neuronal growth *in vitro* with an optimal cell density of 2.0×10^6 cells/ml. An *in vivo* test of the GAE-EngNTs implanted within silicone conduits to bridge a 10 mm gap in rat sciatic nerves for 4 weeks revealed that the constructs significantly promoted axonal regeneration and vascularization across the gap, as compared to the empty conduits although less effective regeneration compared to the autograft groups. *Significance.* Therefore, this is a promising approach for generating anisotropic and robust engineered tissue which can be used with Schwann cells for peripheral nerve repair.

Keywords: dense collagen gel; Schwann cell; nerve regeneration; plastic compression; vascularization

1 Introduction

Peripheral nerve injuries can be debilitating to the quality of life of patients, leading to pain and severe disability. Annually, approximately 200,000-300,000 of patients across the United States and Europe undergo peripheral nerve surgery, with less than half regaining nearly full motor or sensory function [1]. Peripheral nerve transection injuries often result in gaps that must be bridged in order to enable regeneration from the proximal stump to traverse the lesion site and reach the supportive environment of the distal nerve stump. Currently, nerve autografts tend to be used for repairing nerve damage, despite limitations such as donor site morbidity, limited availability and possible size/modality mismatch [2, 3]. The key feature of the nerve autograft, which provides support and guidance to regenerating axons, is the presence of columns of aligned Schwann cells embedded within an anisotropic extracellular matrix (ECM). As a result, researchers in the field of neural tissue engineering have focused on creating structures that mimic the cellular hydrogel structure of the autograft endoneurium. Often this involves the use of natural ECM proteins such as collagen and fibrin [4], combined with Schwann cells or other therapeutic cell types [5] with the ability to provide trophic support to regenerating neurons.

A variety of fabrication strategies have been developed to produce anisotropic engineered tissues using collagen hydrogels [6-9]. This can be achieved using soft, highly-hydrated collagen gels, which make good substrates for cell culture *in vitro,* but tend to have poor mechanical stability and handling properties for implantation *in vivo*. This can be improved by either crosslinking or plastic compression, although these methods can sometimes reduce biocompatibility and affect cell viability [10-13]. Recently, an alternative approach to stabilize collagen gels, called the gel aspiration-ejection (GAE) technique, has been reported [14]. This method exploits negative pressure created within a syringe to draw prefabricated highly-hydrated cellular collagen gels into a cannula, simultaneously imparting compaction and anisotropy on the gels, which are then ejected in a controllable manner. GAE-generated dense collagen gels have been shown to contain highly aligned fibrils that support and sustain mesenchymal stem cell viability and differentiation [14, 15].

The aim here was to investigate, for the first time, whether the GAE technique can be used in nerve tissue engineering, by incorporating Schwann cells to mimic the aligned cellular structure of the

nerve graft. The stability and mechanical properties of the constructs were investigated along with the viability, morphology and distribution of Schwann cells. Having established the methodology to construct stable, robust Schwann cell-loaded engineered neural tissues using GAE (GAE-EngNT), the potential of these constructs in supporting and guiding neuronal regeneration, was assessed both *in vitro* and *in vivo*.

2 Materials and Methods

2.1 Cell culture

A rat-derived Schwann cell line SCL4.1/F7 (Health Protection Agency) was cultured in Dulbecco's Modified Eagle Medium (DMEM; Gibco) and used between passages 4 and 20. *In vitro* neurite growth assays used the NG108-15 rat neuronal cell line (Sigma-Aldrich), which was grown in culture medium (DMEM; Gibco). All media was supplemented with penicillin and streptomycin (100 U/ml and 100 mg/ml, respectively; Sigma-Aldrich) and 10% fetal bovine serum (FBS; Thermo fisher scientific). For both cell types, the cultures were maintained at 37 °C with 5% CO_2, and the media replaced every two days and cells were passaged to maintain them at a sub-confluent level.

2.2 Fabrication of cellular collagen gels and GAE-EngNT

To prepare 1 ml of collagen gel, 100 µl of 10× minimum essential medium (Sigma-Aldrich) was mixed with 800 µl of type 1 rat tail collagen (2 mg/ml in 0.6% acetic acid; FirstLink, UK) and the mixture neutralized using sodium hydroxide before the addition of 100 µl of cell suspension (culture medium containing various cell densities to yield a density in the range $0.5\times10^6 – 4.0\times10^6$ cells/ml of collagen). For GAE-EngNT, 1 ml of this mixture was added to individual wells of a 48-well plate (well diameter = 11 mm, height of the gel = 10 mm) at 4 °C and incubated at 37 °C for 30 min to allow gels to set.

The GAE system consisted of an angioplasty inflation device (AID; B Braun, Germany) connected to a fluid transfer syringe via two Luer lock valves to control the flow direction (Figure 1) [15]. An interchangeable cannula was connected to the distal port of the Luer lock valve. For GAE processing, a flat-ended cannula (diameter ~1.2 mm, gauge 16, VWR International Ltd) attached to the AID was gently inserted half-way into each collagen gel from the top. The piston of the AID was then pulled to create a negative pressure in order to aspirate the collagen gel into the capillary. By continually retracting the piston, the gel was aspirated and lifted from the well plate. Once the gel was almost fully drawn into the cannula (~2.0 mm in length of the gel left from the cannula), the distal Luer lock valve was locked in order to stop the aspiration process and prevent the GAE-EngNT from entering the AID chamber. At this point, positive pressure was applied through the AID to controllably eject rod-shaped GAE-EngNT. GAE-EngNTs were immersed in culture medium and maintained at 37 °C

in a humidified incubator with 5% CO_2/95% air for at least 24 h prior to further analysis. Cell densities were increased via the GAE process in direct proportion to the volume reduction of the gel and final cell density was calculated as initial cell density × fold volume change. Thus, for an initial gel volume of 1 ml, the volume of gel in a 48-well plate was ~950 mm^3 which decreased to ~14 mm^3 following the GAE process, which corresponds to a 68-fold decrease. The cell density would be expected to change from a total of 2.0×10^6 cells/ml to a final cell density of 136.0×10^6 cells/ml.

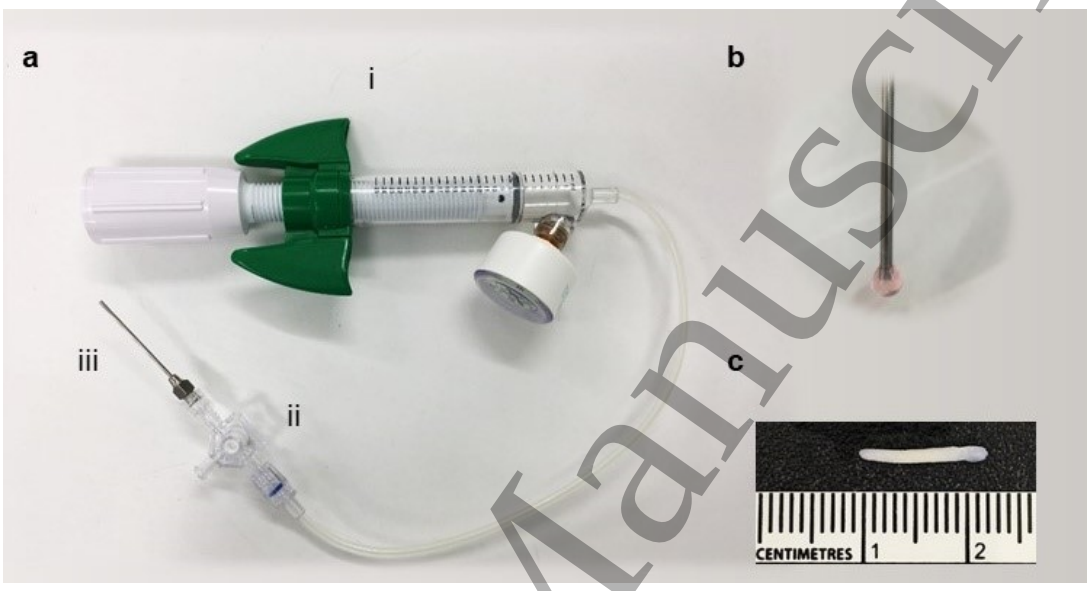

Figure 1. Gel aspiration-ejection system. (**a**) GAE system consisting of: i) an Angioplasty Inflation Device (AID), ii) a Luer lock valve, and iii) a densification cannula. (**b**) Expanded figures showing a precursor hydrated collagen gel during the aspiration process and (**c**) an ejected dense collagen gel from the 16G cannula (with a length of ~12 mm from 1 ml of an initial collagen gel).

2.3 Mechanical testing of GAE-EngNT

Tensile mechanical testing, under both dynamic and quasi-static modes, were performed using a Bose ElectroForce (3200 Series II, TA Instruments) and WinTest 7 Software. GAE-EngNTs were prepared to be at least 10 mm in length and approximately 1.2 mm in diameter (cannula gauge 16) and were placed between the instrument grips with a gauge length of 5 mm. Rat sciatic nerve specimens were tested in an identical manner. Both were assumed to be cylindrical in shape. Samples were kept moist during testing by applying phosphate buffered saline (PBS) to the constructs. To explore the viscoelastic properties, each specimen was subjected to dynamic

mechanical analysis (DMA). In this case, 15% pre-strain was applied to each specimen before the tests. Strain sweep tests were conducted to determine the linear viscoelastic region of deformation, by deforming between 0.05 and 10.00% strain at 5 Hz frequency. Once the strain sweeps were completed, frequency sweep tests from 1-70 Hz were performed in the linear viscoelastic region at 1% strain. The value for the loss tangent (tan δ) was obtained by the ratio of loss modulus E'' (a measure of viscous response of a material) to storage modulus E' (a measure of the elastic response of a material) as shown in an equation below:

$$tan\delta = \frac{E''}{E'}$$

In addition to DMA, samples were subjected to quasi-static tensile testing to failure. Each specimen was stretched at a constant rate of 0.17 mm/s to complete tensile failure in order to obtain stress-strain relationship data. For all constructs, mean ultimate stress, mean ultimate strain, and Young's modulus were determined from the initial length and diameter of the specimens and the force tracings measured during testing. Ultimate tensile stress refers to the amount of force per unit of initial cross-sectional area at tensile failure. Ultimate strain refers to the amount of elongation divided by the initial specimen length achieved at the point of tensile failure. Young's modulus was calculated from the slope of the ascending linear portion of the stress-strain curve.

2.4 Viability of Schwann cells in GAE-EngNTs

Survival of SCL4.1/F7 cells (Health Protection Agency) within GAE-EngNTs was evaluated using the Syto 21/propidium iodide dual-staining assay and the RealTime-Glo luminescent cell viability assay (Promega). Cell viability was measured at 0, 3, 24 and 48 h post-seeding in GAE-EngNTs at an initial density of 0.5×10^6 cells/ml of collagen.

For the Syto 21 (1 mg/ml, Life Technologies)/propidium iodide (PI; 1 mg/ml, Sigma-Aldrich) survival assay, GAE-EngNTs were incubated with PBS containing Syto 21 (diluted 1:1000 in PBS) and propidium iodide (diluted 1:1000 in PBS) for 15 minutes under standard cell culture conditions (37°C, 5% CO_2/95% air). Gels were then washed for 5 min with PBS and repeated six times. The number of live and dead cells was evaluated using a Zeiss AxioLab A1 fluorescence microscope.

For RealTime-Glo cell viability assay (Promega), the MT cell viability substrate (1000X) and NanoLuc® Enzyme (1000X) were added to cell culture medium so that the final concentration of both reagents was a 2X concentration. The 2X RealTime-Glo reagent was then added to the cell culture medium containing GAE-EngNTs at a volume ratio of 1:1 then incubated at 37°C and 5% CO_2/95% air for 1 h. Luminescence was then measured using a microplate reader (Synergy HTX, BioTek) at 1, 3, 24 and 48 h and analyzed via Gen5 software.

2.5 Neurite growth assay

To assess the ability to support neurite outgrowth, either NG108-15 cells (Sigma-Aldrich) or dissociated dorsal root ganglion (DRG) neurons were co-cultured within GAE-EngNTs.

DRG neurons, isolated from adult (200–300 g) Sprague-Dawley rats, were incubated in 0.125% w/v collagenase type IV (Sigma-Aldrich) for 1.5 h at 37 °C. The DRGs were then dissociated by trituration and washed twice with 20 ml of culture medium to achieve a dissociated suspension containing neurons and glial cells (crude DRG). The crude DRG cell suspension was then incubated in DMEM supplemented with 0.01 mM cytosine arabinoside (ara-C; Sigma-Aldrich) in a poly-D-lysine (Sigma-Aldrich) coated flask at 37 °C in a humidified incubator with 5% CO_2/95% air to deplete the glial population. After 24 h, cells were detached using 0.25% trypsin-EDTA solution and centrifuged at 400×g for 5 min. The supernatant was discarded, and the cells re-suspended in the appropriate volume of DMEM (final density was approximately cells from 2 DRG explants suspended in 40 µl media). A dissociated DRG suspension of 40 µl or 100,000 NG108-15 cells were seeded onto the surface of GAE-EngNTs, allowed to settle for 1 h, then constructs were immersed in culture medium (DMEM high glucose, 10% FBS, 1% Pen/Strep) at 37 °C in a humidified incubator with 5% CO_2/95% air. After 3 days, the co-cultures were washed briefly in PBS and fixed in 4% paraformaldehyde at 4 °C for 24 h, and then immunofluorescence staining was carried out.

2.6 Preparation of GAE-EngNT for implantation

Schwann cell-seeded GAE-EngNTs were thoroughly washed in PBS, and then both ends were trimmed to provide a final 10 mm construct length. Each construct was then placed inside a silicone tube (Syndev; 1.57 mm inner diameter, 0.42 wall thickness, 12 mm length) and held in place using

fibrin gel (TISSEEL, Baxter; diluted in DMEM 1:10). Final constructs were kept in cold Hibernate-A medium (Gibco) until implantation *in vivo*.

2.7 Surgical repair of rat sciatic nerve

All surgical procedures were performed in accordance with the UK Animals (Scientific Procedures) Act (1986) / European Directive (2010/63/EU) and approved by the UCL Animal Welfare and Ethics Review Board. Eighteen Spraque Dawley rats (200-250g) were randomized to three groups: GAE-EngNT (n=6), nerve autograft (n=6), empty silicone conduit (n=6). Rats were deeply anaesthetized by inhalation of isoflurane. The left sciatic nerve was exposed at mid-thigh level, transected to create a 10 mm gap and then repaired either by rotation and replacement of the tissue (autograft) or insertion of the proximal and distal nerve stumps 1 mm into the 12 mm tube, in each case securing with two epineurial sutures (Ethilon 10/0; Ethicon-Johnson & Johnson, Brussels) at each stump. Wounds were then closed in layers and animals were allowed to recover for 4 weeks, then culled using CO_2 asphyxiation before nerves were harvested and fixed using 4% paraformaldehyde overnight at 4ºC.

2.8 Preparation of nerves for histological analysis

Fixed nerves were washed thoroughly with PBS. Nerves were incubated in 15% sucrose in PBS for ~30 min until tissues became submerged and then transferred to 30% sucrose in PBS overnight at 4 ºC. Nerve samples were then dissected into pieces for further analysis as shown in Figure 2. The segments were then incubated for 2-4 h at RT in 1:1 v/v 30% sucrose in PBS: optimal cutting temperature (OCT; Leica) solution. Samples were embedded in that 1:1 mixture in a cryosection mould (TAAB) and snap-frozen in liquid nitrogen before storage at -80 ºC.

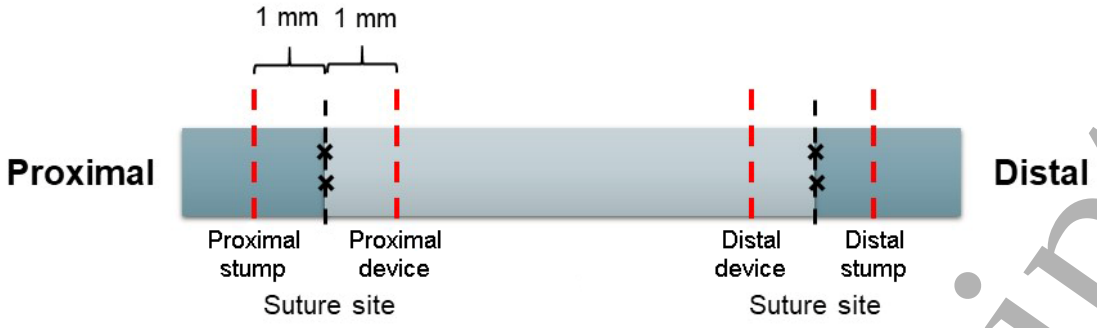

Figure 2. Schematic diagram of the nerve tissue preparation.

Transverse sections (15 µm thick) were prepared from the proximal and distal stumps, at defined distances into the nerve stumps from the injury site, using a cryostat (Leica CM1860). The sections were adhered to glass slides (Superfrost TM Plus, Thermo Fisher Scientific) for histological analysis. The transverse sections that were used for analysis were from positions 1 mm into the proximal and distal stumps, or 1 mm into the proximal and distal parts of the repair site, measured from the repair boundaries (suture sites) in each case (Figure 2).

2.9 Immunofluorescence staining

Nerve sections were washed in PBS three times for 5 min each wash. They were then permeabilized using 0.3% Triton X-100 (Sigma-Aldrich) for 30 min, blocked using 10% goat serum (GS) for 1 h, and then incubated in primary antibodies (Table 1) overnight at 4 °C. All antibody dilutions were performed in 10 % goat serum. The following day, tissue sections were washed three times for 5 min in PBS then incubated with appropriate DyLight-conjugated secondary antibodies at room temperature for at least 1 h in a dark humidified chamber. Finally, sections were washed three times with PBS for 5 min each wash and mounted using VECTASHIELD Hard-set Mounting Medium with DAPI (Vector Laboratories).

GAE-EngNTs from *in vitro* studies were fixed in 4% paraformaldehyde in PBS for 24 h at 4 °C, washed twice for 10 min with PBS, and then permeabilized in 5% Triton X-100 for 30 min at room temperature. Gels were then washed three times with PBS for 10 min each followed by incubating with 5% GS for 30 min at room temperature to block non-specific binding. Primary antibody (Table 1) was diluted in PBS and gels were incubated overnight at 4 °C. The following day the gels were

washed six times for 5 min each wash in PBS and incubated with secondary antibody in PBS (1:250) for 90 min at room temperature then washed again with PBS. Finally, gels were stained with Hoechst 33342 (1:1000) for 5 min at room temperature and washed once more with PBS for 5 min.

Table 1. Antibody manufacturers, dilutions and incubation times.

Antibody	Brand	Dilution	Incubation
S100	DAKO	1:400	Overnight 4°C
Neurofilament	Eurogentec	1:1000	Overnight 4°C
βIII-tubulin	Sigma-Aldrich	1:400	Overnight 4°C
RECA-1	Bio-rad	1:100	Overnight 4°C
DyLight 488 anti-Mouse	Thermo Fisher	1:250	90 min Room temperature
DyLight 549 anti-Rabbit	Thermo Fisher	1:250	90 min Room temperature

2.10 Microscopy and image analysis

All fluorescence images of Schwann cells, axons and blood vessels were acquired using confocal microscopy (Zeiss LSM 710). Neurite images were obtained from a Zeiss AxioLab.A1 inverted fluorescence microscope.

For the gel contraction measurement, GAE-EngNTs and highly-hydrated collagen gels were imaged as made (0 h) and at 24 h. Images were analyzed using ImageJ software to determine the area of the gels, and contraction at 24 h calculated as a percentage of initial gel area.

For the analysis of Schwann cells in GAE-EngNTs, three z-stacks were randomly selected from the middle region of each gel. The imaging volume of 424.85 μm × 424.85 μm × 104.36 μm with a voxel

size of 0.244 µm × 0.244 µm × 4.348 µm (20x magnification) was captured and flattened into a single z-stack. For each experiment, the same volume and number of z-stacks were taken, and the same acquisition settings were used. The alignment, length and shape factor measurements were analyzed in 3D using Volocity™ software (Perkin Elmer, Waltham, MA). Length of neurites was analyzed using the Simple Neurite Tracer plugin in ImageJ software. Data were collected from the whole gel in three experimental replicates.

For the analysis of axon growth *in vivo*, high contrast tile-scan confocal micrographs were used to quantify all the neurofilament positive axons present in each section. Counting was performed via Volocity™ software. The protocol settings remained consistent for each confocal micrograph. For each location within each nerve sample, three tissue sections were analyzed. For the analysis of blood vessels *in vivo*, ImageJ software was used to count and measure the diameter of blood vessels in sections (three tissue sections measured per condition from 6 separate animals).

2.11 Statistical analysis

A Kolmogorov-Smirnov normality test was performed to confirm whether data were normally distributed. Data were then analyzed using a one-way ANOVA or two-way ANOVA with a significance level of 0.05, followed by Dunnett's or Tukey's multiple comparisons post hoc test.

3 Results

3.1 GAE-EngNTs exhibit similar viscoelastic behaviors to rat sciatic nerves

Tensile DMA was performed to compare GAE-EngNTs to freshly harvested rat sciatic nerve tissue. Figure 3a shows the strain sweep used to determine the linear viscoelastic region, which indicated that strain should be applied below 1%. GAE-EngNTs and nerve tissue exhibited similar behavior during strain sweep tests, with each having an equivalent linear viscoelastic region.

To test viscoelastic behavior, frequency-dependent sweep tests were conducted at a constant strain of 1% (Figure 3b). The values for storage modulus (E') dominate over loss modulus (E'') which indicates inherent high elastic properties. All GAE-EngNTs showed a tan δ ~ 0.2 and a slight frequency dependence (Figure 3c), which is usually an indicator of a strong and stable elastic gel [16]. This was similar to the rat sciatic nerve tissue, although the elastic modulus of the nerves was slightly higher than that of the GAE-EngNTs. GAE-EngNTs exhibited greater variability of tan δ at higher frequencies compared to the rat sciatic nerves indicating relatively inconsistent structural integrity of the gels [17].

Tensile testing to failure was conducted to determine the Young's modulus and overall strength of materials. The ultimate strain of GAE-EngNTs was approximately 0.681, which was slightly lower than that of rat sciatic nerves (0.883) (Figure 3d). However, the ultimate stress of GAE-EngNTs and Young's modulus beyond 0.5 (50%) strain were considerably less than that of rat sciatic nerve tissue.

At low strains of less than 1% (viscoelastic region), the GAE-EngNT exhibited similar mechanical properties to the rat sciatic nerve whereas beyond around 50% strain the nerve was much stronger and stiffer (Table 2).

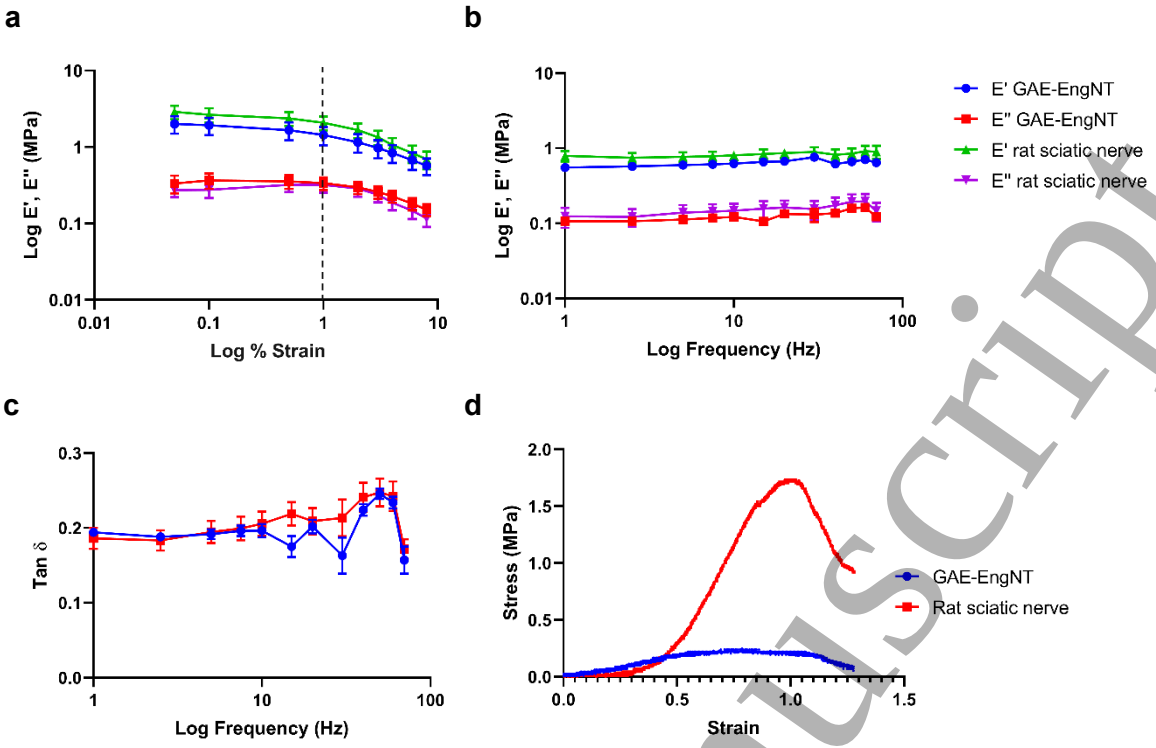

Figure 3. Mechanical properties of GAE-EngNTs and rat sciatic nerves. (**a**) Initial tensile DMA strain sweeps were performed at 5 Hz to determine the linear-viscoelastic limit. Both viscous and elastic components, shown respectively as the storage (E') and loss (E'') moduli (MPa) were determined from 0.05 to 8% strain for both GAE-EngNTs and rat sciatic nerves. (**b**) Frequency sweeps were conducted at 1% strain from 1-70 Hz. The loss tangent (tan δ) is shown in (**c**). Data are shown as mean ± SEM, n=5. (**d**) Representative stress-strain relationship for GAE-EngNTs and rat sciatic nerves.

Table 2. **The storage, loss modulus, ultimate stress, ultimate strain and Young's modulus of the GAE-EngNTs and rat sciatic nerves.** For the storage and loss modulus, data were obtained at 5 Hz and 0.05 -1.00% strain (linear viscoelastic region). Data are shown as mean ± SD. n=5. For the ultimate stress, ultimate strain and Young's modulus, data were obtained from tensile tests under a strain rate of 0.17 mm/s. Mean data were calculated from the stress-strain curves in which the tensile Young's modulus was calculated from the slope of the initial linear part of the curve. Data represent mean ± SD. n=7.

Group	E' (MPa)	E'' (MPa)	Ultimate stress (MPa)	Ultimate strain	Young's modulus (MPa)
GAE-EngNT	1.764±0.261	0.349±0.015	0.219±0.070	0.681±0.212	0.351±0.151
Rat sciatic nerve	2.500±0.347	0.298±0.026	1.776±0.383	0.883±0.176	3.523±0.728

3.2 GAE-EngNTs are stable and can support and maintain Schwann cell viability and alignment

To determine the ability of the GAE-EngNTs to resist deformation as a result of cell-matrix interaction, gel contraction *in vitro* was examined. The contraction profile of Schwann cells within GAE-EngNTs over a range of four initial cell densities: 0.5, 1, 2 and 4×10^6 cells/ml of collagen was quantified. After 1 day in culture, media was removed from gels, images were captured and the percentage contraction was calculated from the area of each gel at 24 h compared to the original area at 0 h. Data were compared to the contraction profile for Schwann cells in standard 2 mg/ml highly-hydrated collagen gels using a 96-well plate assay as a control [18].

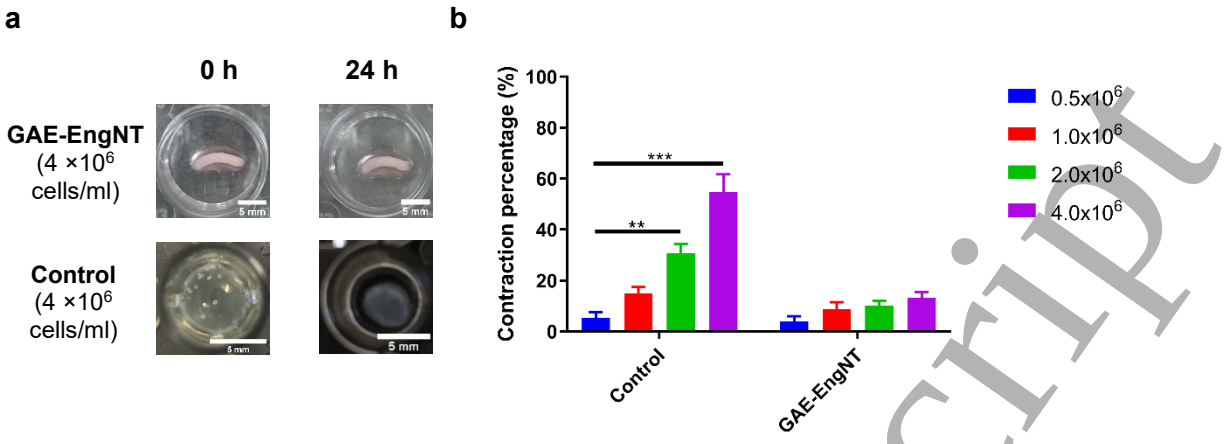

Figure 4. Stability of cellular GAE-EngNTs *in vitro*. (**a**) Representative images of GAE-EngNTs and standard 2 mg/ml highly-hydrated collagen gel controls. (**b**) The standard collagen gel controls showed cell-density dependent contraction, whereas GAE-EngNT contraction was minimal. Data are mean ± SEM. n=5. ***P=0.001, **P=0.0083 by two-way ANOVA with Dunnett's test for comparison with the respective 0.5×10^6 cells/ml group. Scale bars, 5 mm.

It can be seen from Figure 4 that there was a minimal contraction in the GAE-EngNTs compared to the standard highly-hydrated collagen gels. Even with the highest starting cell density of 4×10^6 cells/ml, the contraction of GAE-EngNTs was below 20% and not significantly different from the contraction of gels with the lowest cell density, whereas highly-hydrated gels showed significant cell-density-dependent contraction.

Live/dead staining using propidium iodide indicated that the GAE technique resulted in approximately 24% cell death, whereas there was about 10% cell death in highly-hydrated gels at 0 h (Figure 5). At later time points, the % cell death reduced, becoming comparable to the control by 24h. Similarly, the metabolic activity of cells within GAE-EngNTs was half that in control gels immediately after GAE, then increased to approximately 66% of control from 3 to 48 h, with no substantial loss in activity over time *in vitro* (Figure 5).

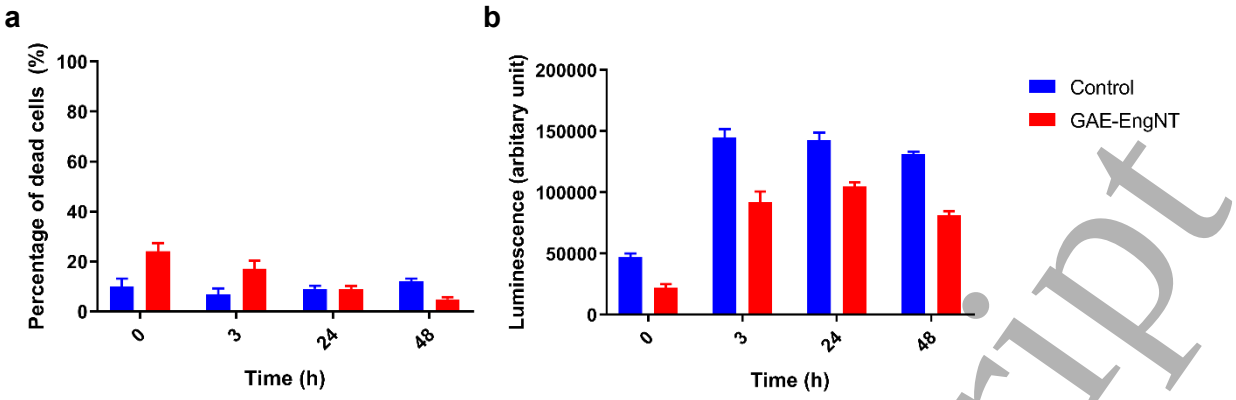

Figure 5. Cell viability assessment using RealTime-Glo assay and PI-Syto21 staining. (**a, b**) Cell viability was determined by PI and Syto 21 and RealTime-Glo assay. Schwann cells (F7) at an initial density of $0.5x10^6$ /ml collagen gel were seeded in GAE-EngNTs, and controls were standard 2mg/ml highly-hydrated collagen gels in 96-well plates. Data are means ± SEM, n=3.

The effect of GAE on the alignment of Schwann cells was investigated by studying the cells in different regions of the gels and at different times after manufacture. The different gel regions were classified according to their position along the length of the cylindrical GAE-EngNT (Figure 6a). Schwann cells were aligned longitudinally, parallel with the long axis of the gel, throughout the construct, but length and alignment were greater in the regions that were aspirated first compared with the leading end which was aspirated later (Figure 6b). Figure 6c shows that Schwann cells remained aligned and became more elongated as a function of time in culture, *in vitro*.

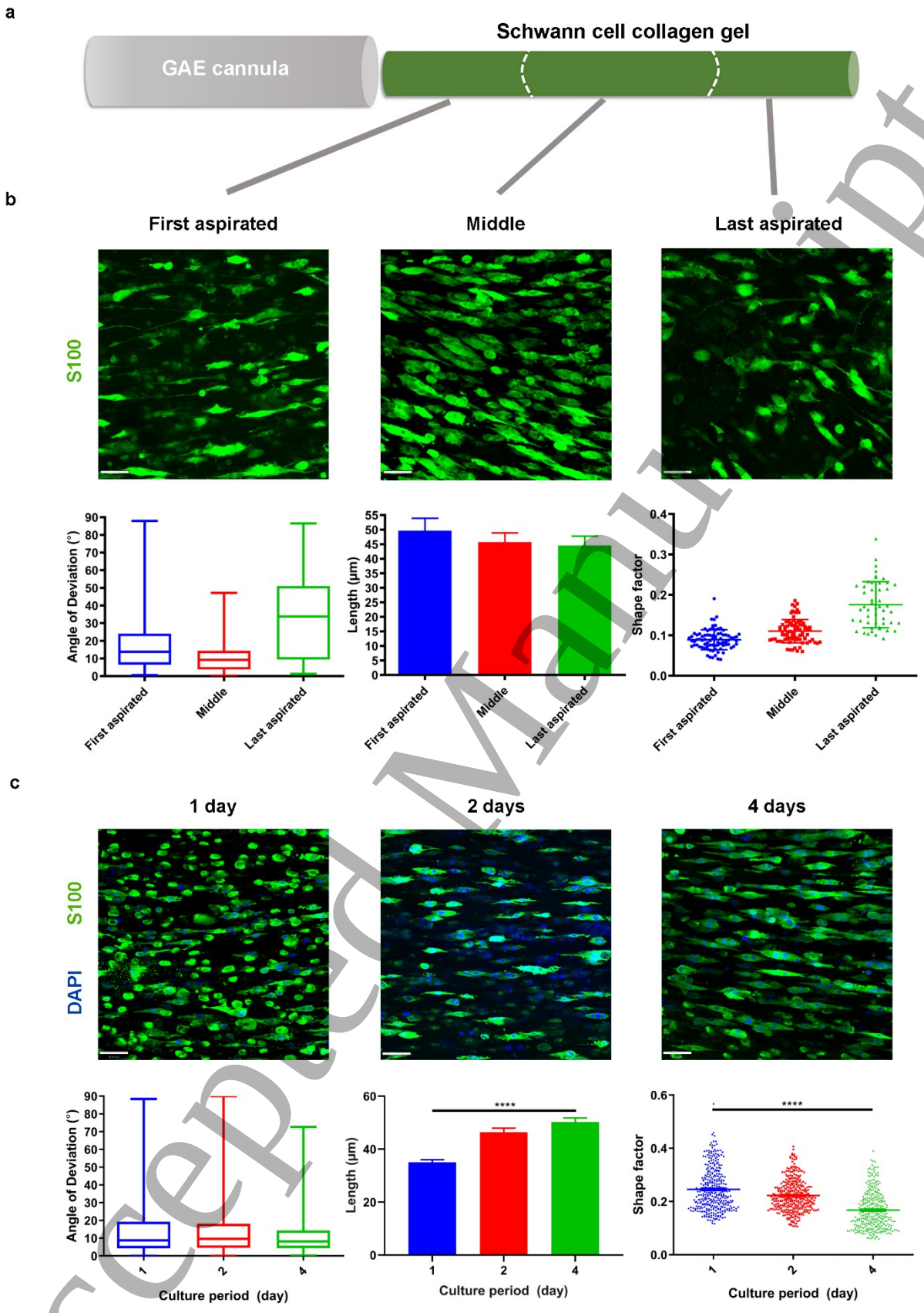

Figure 6. Schwann cells elongate and align within GAE-EngNTs. (**a**) Schematic diagram showing the positions of regions analyzed (2 mm of the first aspirated region, 6 mm of the middle region, and 2 mm of the last aspirated region). (**b**) Representative confocal z-stack micrographs show Schwann cells in three different regions (first aspirated, middle and last aspirated). Schwann cells were seeded at an initial density of $0.5x10^6$ /ml gel for GAE. Corresponding quantification of the angle of deviation, length and shape factor (a value closer to 1 indicates a more rounded object) are shown. (**c**) Representative confocal micrographs of Schwann cells at different time points in culture. Angle of deviation, length and shape factor were plotted. Box plots show lower and upper quartile and median, whiskers show min and max. Other data are shown as mean ± SEM. n=337 cells from 3 independent experiments. ****P<0.0001 by one-way ANOVA with Tukey's multiple comparisons test. Scale bars, 52 μm.

3.3 GAE-EngNTs containing aligned Schwann cells support neuronal regeneration *in vitro*

Co-cultures were established by seeding NG108-15 cells on to the surface of cellular GAE-EngNTs (Figure 7). GAE-EngNTs containing aligned Schwann cells supported and guided neuronal growth in a cell-density-dependent manner, with a 2.4-fold increase in neurite length detected where GAE-EngNTs were made using Schwann cells at a higher initial cell density. Similar NG108-15 neurite extension was detected with GAE-EngNTs made using Schwann cells at initial densities of 4×10^6 cells/ml and 2×10^6 cells/ml (Figure 7a and 7b). This was also observed when the co-culture experiment was conducted using DRG neurons (Figure 7d and 7e). Therefore, an initial seeding density of 2×10^6 cells/ml was used for generating GAE-EngNTs in the subsequent *in vivo* analysis. Neurites from both NG108-15 cells and DRG neurons were shown to significantly align along the Schwann cell GAE-EngNTs (Figure 7c and 7f).

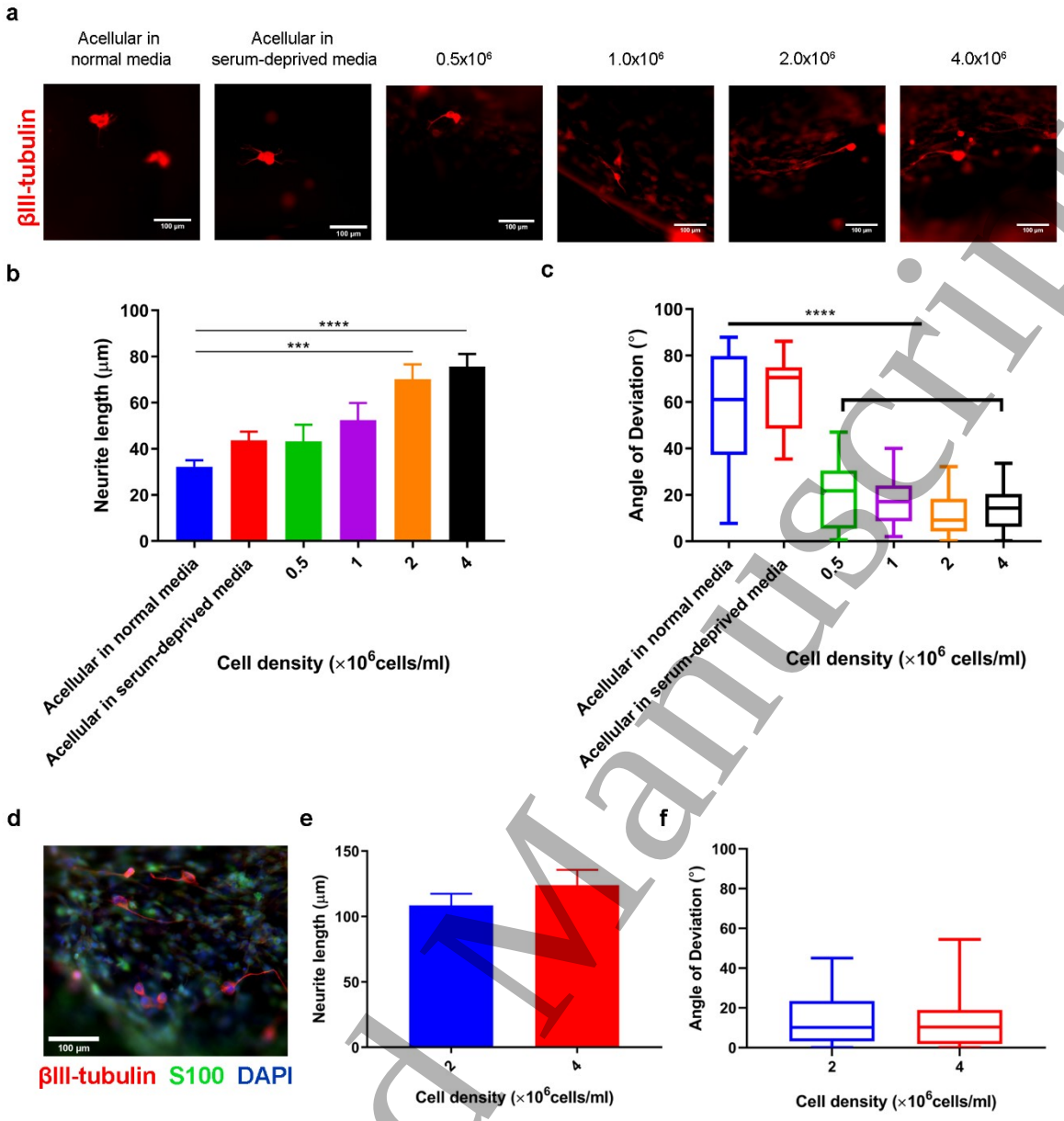

Figure 7. Neuronal outgrowth evaluation using NG108 and DRG co-culture assay. (**a**) Representative fluorescence images of NG108-15 cells seeded onto the surface of GAE-EngNTs containing no cells or different initial seeding densities of F7 Schwann cells for 3 days. Image analysis was used to calculate neurite length (**b**) and orientation in relation to the long axis of the GAE-EngNT (**c**). Additional experiments were conducted using DRG neurons seeded onto the surface of GAE-EngNTs made using the two highest densities of F7 Schwann cells (**d, e, f**). Whiskers show min and max and the box shows the inter-quartile range and median. Data are mean ± SEM, n=40 cells from 3 independent experiments. ****P<0.0001, ***P=0.0001 by one-way ANOVA with

Dunnett's test for comparison with the respective acellular in the normal media group. Scale bars, 100 μm.

3.4 GAE-EngNTs containing aligned Schwann cells support neuronal regeneration in a rat sciatic nerve injury model

A 10 mm gap rat sciatic nerve model was used to compare three surgical treatment groups: GAE-EngNTs, empty conduits and autografts, with the histological assessment after 4 weeks of recovery.

Repaired nerves were dissected and analyzed using transverse sections through the proximal and distal end of the repair site and proximal and distal stumps (Figure 8). In all groups, the number of neurites decreased with distance distally. All groups showed a similar number of axons in the proximal stumps, with fewer than half the number of axons present in the proximal device part of the empty tube controls compared to that of the nerve autografts controls. In the distal device region and the distal stumps of the empty tube groups, there was minimal regeneration, suggesting that this 10 mm gap rat model with 4-week postoperative time mimics the poor regeneration seen in critical size 'long-gap' repair in humans. The GAE-EngNT groups supported 8-fold more axons than the empty tube controls in both the distal device and distal stump, although this was significantly fewer than in the nerve autograft groups.

a

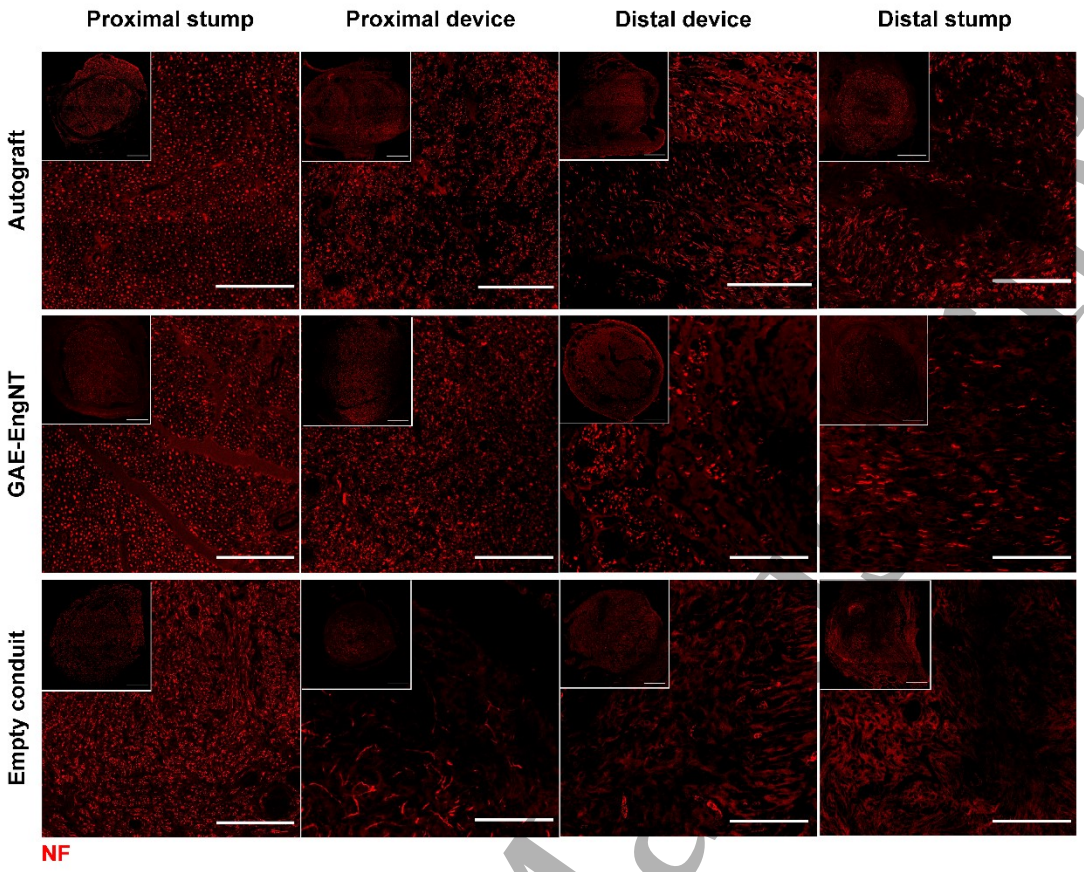

b

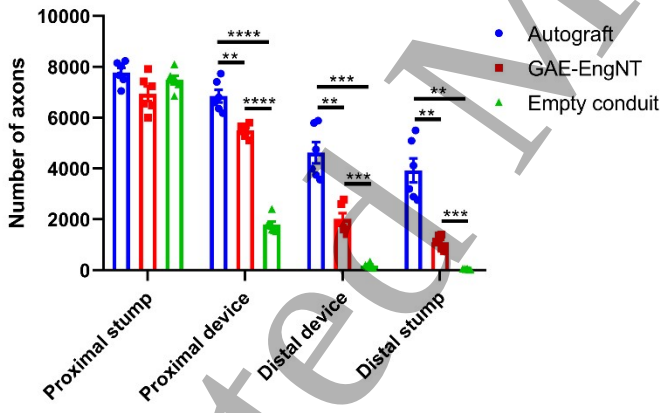

c

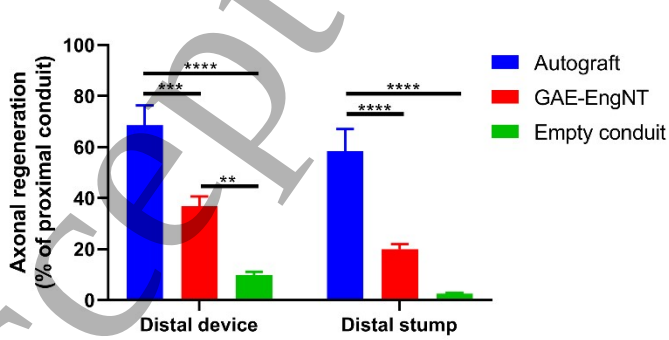

Figure 8. GAE-EngNT containing aligned Schwann cells supports regeneration across a 10 mm repair and into the distal stump. (**a**) Representative confocal micrographs of transverse sections showing neurofilament positive neurites at four different positions in the repaired nerves; the proximal stump, proximal device, distal device and distal stump. Scale bars, 100 μm. Insets show lower magnification views of the whole cross-sections (scale bars 200 μm). (**b**) Quantification of the total number of neurofilament-positive axons per transverse section at the four different positions across the repair sites. (**c**) Axons in the distal device and distal stump expressed as a percentage of the number of axons in the proximal part of the device in each case. Data are mean ± SEM. n=6. Two-way ANOVA showed significant differences between the three treatment groups ($P<0.0001$), the four sampling positions ($P<0.0001$) and the interaction between them ($P<0.0001$). Tukey's multiple comparisons post hoc test was used to compare the three treatment groups at each sampling position and significant differences are indicated as *P<0.05, **P<0.01, ***P<0.001, ****P<0.0001.

The vascularization of the implanted GAE-EngNT constructs was examined via immunohistochemical staining of transverse sections using RECA-1 and compared to the autograft and empty conduit groups (Figure 9). The GAE-EngNT groups showed comparable numbers of blood vessels to the nerve autograft controls, whereas there were significantly fewer blood vessels in proximal regions of the empty tube controls. There were no significant differences in the diameter of blood vessels between different locations and groups (Figure 9c).

a

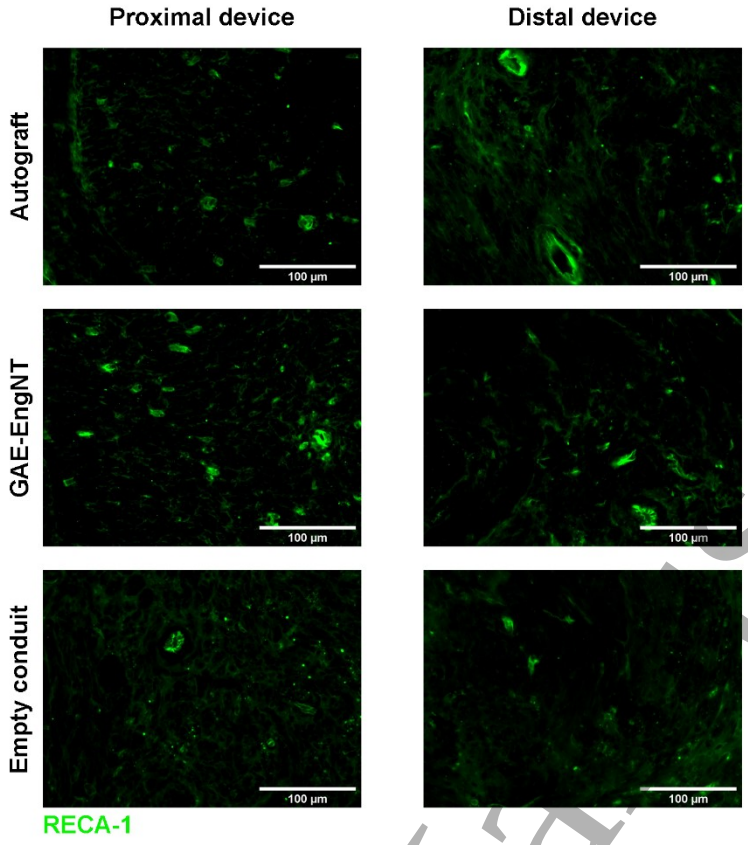

b

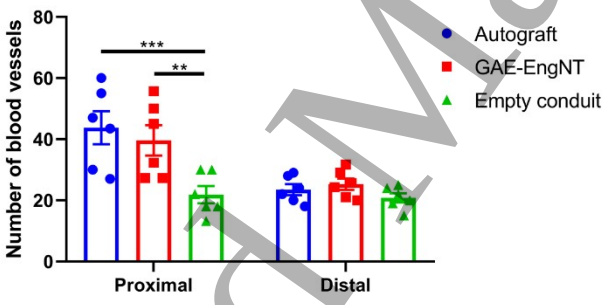

c

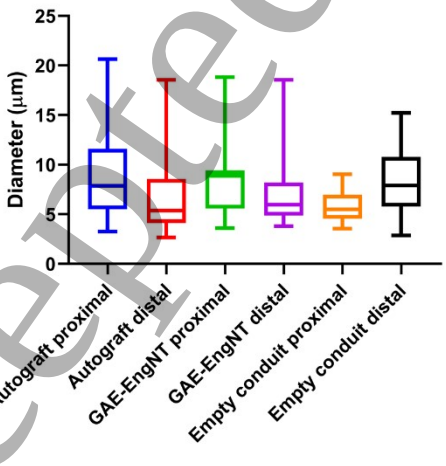

Figure 9. Vascularization of GAE-EngNTs following rat sciatic nerve repair. (**a**) Representative fluorescence images of RECA-1 positive blood vessels in transverse sections from the proximal device and distal device positions, 4 weeks following repair of 10 mm rat sciatic nerve gap. (**b**) Number and (**c**) diameter of blood vessels at each location. Box plots show min, max and median, with lower and upper quartile. Data are mean ± SEM. n=6. Two-way ANOVA with Tukey's multiple comparisons post hoc test revealed a significant difference ($P<0.001$) in the number of blood vessels between the proximal and distal position and significant differences between groups in the proximal device, ***$P<0.001$, **$P<0.01$.

4 Discussion

This study showed for the first time that the gel aspiration-ejection (GAE) technology can be used to generate compact, mechanically stable collagen hydrogels containing aligned columns of Schwann cells within an aligned collagen matrix. This closely mimics key features important for supporting nerve regeneration and resembles the columns of elongated aligned Schwann cells in the Bands of Büngner and our previously reported EngNT [6]. However, unlike the EngNT method of cellular self-alignment followed by plastic compression, GAE offers a more efficient and rapid route of generating aligned cellular gels in one step with around 15 min, as compared to the EngNT method which normally takes at least 24 h. Furthermore, the GAE-EngNTs can be immediately cylindrical whereas EngNT sheets must be rolled to resemble nerve tissue. Through the application of pressure differentials, GAE-EngNTs can be produced with tunable collagen fiber densities and mechanical properties [15], and recent studies have shown that the approach can be automated [19]. Here, the cannula gauge and volume of initial gel was optimized to enable GAE-EngNTs with appropriate size and shape to mimic nerve tissue to be produced. Tensile DMA indicated that GAE-EngNTs had a similar range of linear viscoelastic region (LVR) to a rat sciatic nerve, which is around 1.0% strain. Soft biological tissues such as the brain and liver also have a LVR around 0.1-1% [20-23]. A frequency sweep to examine the viscoelastic properties of the material indicated that the hydrogels displayed consistent and predominantly elastic behavior, as both E’ (storage modulus) and E’’ (loss modulus) were minimally affected by frequency changes over the investigated range [24]. This is consistent with the study done by C. Kayal from RAFT-stabilized collagen gels [25]. Also, E’ appeared to be around 5 times higher than E” showing a similar behavior to a previous study which reported that E’ was 10 times greater than E’’ for human ulnar nerves [26]. Furthermore, tan δ; the ratio of the storage and loss moduli, remained largely constant at around 0.15-0.25, further indicating dominant elastic behavior under load [16]. The DMA results for GAE were similar to those of rat sciatic nerves suggesting that GAE-EngNTs exhibit comparable viscoelastic behaviors to natural nerve tissue.

According to the stress-strain curve generated during the tensile test to failure, the elastic modulus of GAE-EngNTs is around 0.35 MPa, which is higher than that reported for fully hydrated collagen

gels (1.5 kPa - 0.14 MPa) [27-29]. Plastic compressed hydrogels were shown to have Young's modulus of around 2.2 MPa (following 96-97% fluid loss) which is significantly higher than that of their original highly-hydrated ones (~2.1 kPa) [25, 30, 31]. However, our values for ultimate stress (~0.22 MPa) and ultimate strain (~0.68) correspond to previous reports for aligned collagen hydrogels (ultimate stress ~0.3-0.6 MPa and ultimate strain ~0.30 - 0.55), produced via either biaxial or uniaxial compression [32]. The tensile mechanical properties of rat sciatic nerves tested in this study were consistent with those reported by G. H. Borschel [33]. The ultimate strain of the GAE-EngNTs was similar to the fresh sciatic nerve, but their ultimate strength and Young's modulus were lower. The higher strength of native nerves is largely attributable to the dense layers of perineurial cells and collagen fibrils within the perineurium as well as thicker longitudinally distributed collagen fibrils in the epineurium [34]. Nonetheless, the mechanical properties of GAE-EngNTs were similar to the endoneurium of rat sciatic nerves in terms of tensile strength and Young's modulus [35]. This indicates that GAE-EngNTs are mechanically suitable for use as the inner component of an artificial nerve conduit, but these may ultimately require strong outer sheath materials that match the mechanical properties of the epineurium in order to match overall nerve mechanical features.

GAE-EngNTs containing Schwann cells were stable *in vitro* and resisted the cell-mediated contraction associated with highly-hydrated control gels [18]. Previous reports have shown that the viability of fibroblasts and mesenchymal stem cells was maintained within GAE gels *in vitro* [14, 15], and this study confirmed that Schwann cells could survive the process. Schwann cells subjected to GAE showed similar survival to cells in 2 mg/ml highly-hydrated collagen control gels. The percentage of dead cells in GAE-EngNTs reduced over 2 days, likely due to increased cell proliferation over time as shown previously with mesenchymal stem cells in GAE gels [15]. In general, the metabolic activity of cells within GAE-EngNTs was lower than in control gels. In other studies, the process of cell injection has been linked with adverse effects [36], perhaps due to shear stress and pressure. However, in the absence of cell death, a reduced metabolic activity might be beneficial for cells to survive under hypoxic conditions following implantation [37]. The diffusion of oxygen through dense stabilized collagen materials generated using plastic compressed has been shown previously to be within the normal physiological range of native tissue [38], indicating that the

diffusion of oxygen through GAE-EngNTs is not likely to be a limiting factor influencing cell viability and metabolic activity although it would be interesting to investigate this further.

Cell morphology and alignment characterization revealed that the majority of aligned Schwann cells were present in the middle region whereas those near the ends of the constructs were more randomly oriented. Interestingly, in the first aspirated region, cells seemed to be more aligned than in the last aspirated region. This difference in elongated morphology may reflect the different forces that cells experience at the various stages of aspiration and ejection. Cells that were in the part of the gel aspirated first will have travelled further within the cannular and therefore been exposed to the resultant forces over a longer duration than the cells in the last part of the gel to enter, which may have influenced the morphology [39]. Understanding the mechanism by which the forces generated within a gel during GAE confer elongation and alignment on cells within the gel would be an interesting topic for future study and may lead to further improvements in cellular architecture. Importantly, the alignment conferred on the Schwann cells during the GAE process was maintained throughout the 4 days of subsequent culture duration, and indeed the length of the Schwann cells slightly increased when cultured for longer periods, indicating a sustained orientation effect.

NG108-15 cells and adult rat DRG neurons extended highly aligned neurites parallel to the Schwann cell orientation in GAE-EngNTs, suggesting the ability of the constructs to provide neuronal guidance and support. This was a cell density-dependent effect with longer neurites associated with greater numbers of Schwann cells within GAE-EngNTs. Establishing the optimal seeding cell density is important in nerve tissue engineering to reduce costs and because Schwann cell density affects cell survival, proliferation, differentiation and extracellular matrix synthesis, all of which can influence nerve regeneration [40-42]. The *in vitro* data reported here indicated that 2×10^6 Schwann cells/ml was an optimal starting density. This resulted in a final cell density of 136×10^6 cells/ml in GAE-EngNTs, which is a 68-fold increase relative to the density in highly-hydrated gels. This fold increase was also considered to be higher than in single-plastic compressed collagen gels (58-fold increase), used to produce EngNT [6, 43].

A 10 mm gap rat sciatic nerve model with a recovery period of 4 weeks was used to explore the ability of GAE-EngNTs to support nerve regeneration. This combination of gap length and timepoint

have been used in several previous studies [44-49], and the results here confirm that this is a good model for testing engineered tissues since there was a clear difference in neurite growth through an empty tube compared to an autograft. Very few neurites successfully entered and extended across the gaps in the empty tube control group, whereas other studies have reported greater regeneration through 10 mm silicone tubes [50], the disparity likely resulting from differences in duration and method of outcome measurement. The aligned cellular GAE-EngNTs supported more neurite growth than the empty tube controls, but not to the same extent as the autograft. This is not dissimilar to previous studies using other types of tissue-engineered constructs [6, 51] and indicates that with some optimization in terms of the cell and collagen density, the GAE approach to generating aligned cellular collagen could be an effective way to make nerve repair constructs.

Vascularization of nerve grafts is essential to provide nutrients and blood supply to the implanted cells, improving their survival and encouraging regeneration [52]. Several previous studies have shown that the primary method of revascularization of nerve grafts involves inosculation, which occurs from the anastomosis of host and graft tissue vasculature [53-55]. When compared to a previous study using EngNT to repair rat sciatic nerves, GAE resulted in the ingrowth of a slightly higher number of vessels, which could imply this type of construct supports greater vascularization, although further experiments would be required to test that hypothesis [56]. The number and diameter of blood vessels shown in our study were similar to those reported previously for native rat sciatic nerve, further supporting the conclusion that adequate vascularization was promoted in the GAE-EngNT constructs [57, 58].

It should be noted that the F7 rat Schwann cell line was used throughout the study as a model cell type because of their ease of use, consistency, and reproducibility. This model Schwann cell line is well characterized and has been shown to retain key molecular features of rat Schwann cells and to remain viable when implanted into rats, supporting regeneration and myelination of neurons with no adverse effects in terms of stability and malignancy [6, 51, 59]. Having used these cells to test the GAE concept for nerve repair, further studies can now explore the combination of the GAE system with primary Schwann cells, stem cell-derived Schwann cells, or other potentially therapeutic cell types for use in translational nerve tissue engineering.

Recently, the GAE system has been automated, an important step towards enabling the future production of clinical grade engineered tissue at scale [19]. In its current form GAE-EngNT lacks the tensile strength to be used independently in nerve grafting and was therefore delivered within a silicone tube. This is not a suitable solution for use in human patients due to silicone being mechanically mismatched with nerve tissue and non-biodegradable. To overcome this limitation, future research will need to explore whether GAE-EngNT could be manufactured with improved strength, for example by generating density gradients within the structures, or delivered within alternative biomaterials that are more biocompatible, biodegradable, and exhibit epineurium-like mechanical properties. Furthermore, the interfaces between the GAE-EngNT and the proximal and distal nerve stumps should be optimized to boost proximal ingrowth and prevent axon entrapment within the supportive graft environment [60]. It would be interesting to explore this further by examining longitudinal sections through the repair site in future experiments, which could also involve different time points and longer gap lengths to build up a detailed understanding of how regenerating axons progress through the constructs from proximal to distal nerve stump.

Overall, the results of this study show for the first time that the GAE approach can be applied in nerve tissue engineering. Cylindrical constructs containing aligned Schwann cells in a compacted, mechanically stable collagen matrix were generated rapidly and shown to be effective in supporting neuronal growth *in vitro* and *in vivo*. The simplicity and suitability of this approach for automation and scale up make it a powerful new tool for the translation of neural tissue engineering to clinical nerve repair. Future work will focus on optimizing the GAE-EngNTs to improve efficacy, which will be tested in preclinical models of nerve injury repair using longer gaps and later time points combined with functional outcome measures.

5 Conclusions

The gel aspiration-ejection technique can be effectively applied to peripheral nerve tissue engineering as a rapid and robust method to generate anisotropic cellular collagen gels with controllable size, defined mechanical properties, and nerve-like cylindrical geometry. GAE-EngNTs containing aligned Schwann cells were able to support and guide neuronal growth both *in vitro* and *in vivo,* demonstrating the potential for this approach to be used in the construction of nerve repair conduits.

Acknowledgements

The authors would like to acknowledge the Royal Thai Government Scholarship and funding of Canada NSERC, FRQNT and McGill's Faculty of Engineering for the MEDA fellowship to HP.

Conflict of interest

The authors have no conflict of interests.

References

[1] Ichihara S, Inada Y and Nakamura T 2008 Artificial nerve tubes and their application for repair of peripheral nerve injury: an update of current concepts *Injury* **39** 29-39

[2] Palispis W A and Gupta R 2017 Surgical repair in humans after traumatic nerve injury provides limited functional neural regeneration in adults *Exp Neurol* **290** 106-14

[3] Arslantunali D, Dursun T, Yucel D, Hasirci N and Hasirci V 2014 Peripheral nerve conduits: technology update *Med Devices (Auckl)* **7** 405-24

[4] Brown R A and Phillips J B 2007 Cell responses to biomimetic protein scaffolds used in tissue repair and engineering *Int Rev Cytol* **262** 75-150

[5] Bhangra K S, Busuttil F, Phillips J B and Rahim A A 2016 Using Stem Cells to Grow Artificial Tissue for Peripheral Nerve Repair *Stem Cells Int* **2016** 7502178

[6] Georgiou M, Bunting S C, Davies H A, Loughlin A J, Golding J P and Phillips J B 2013 Engineered neural tissue for peripheral nerve repair *Biomaterials* **34** 7335-43

[7] Walters B D and Stegemann J P 2014 Strategies for directing the structure and function of three-dimensional collagen biomaterials across length scales *Acta Biomater* **10** 1488-501

[8] Park H, Cannizzaro C, Vunjak-Novakovic G, Langer R, Vacanti C A and Farokhzad O C 2007 Nanofabrication and microfabrication of functional materials for tissue engineering *Tissue Eng* **13** 1867-77

[9] Phillips J B, Bunting S C, Hall S M and Brown R A 2005 Neural tissue engineering: a self-organizing collagen guidance conduit *Tissue Eng* **11** 1611-7

[10] Cheema U and Brown R A 2013 Rapid Fabrication of Living Tissue Models by Collagen Plastic Compression: Understanding Three-Dimensional Cell Matrix Repair In Vitro *Adv Wound Care (New Rochelle)* **2** 176-84

[11] Lai E S, Anderson C M and Fuller G G 2011 Designing a tubular matrix of oriented collagen fibrils for tissue engineering *Acta Biomater* **7** 2448-56

[12] Mi S, Chen B, Wright B and Connon C J 2010 Plastic compression of a collagen gel forms a much improved scaffold for ocular surface tissue engineering over conventional collagen gels *J Biomed Mater Res A* **95** 447-53

[13] Zeugolis D I, Paul G R and Attenburrow G 2009 Cross-linking of extruded collagen fibers--a biomimetic three-dimensional scaffold for tissue engineering applications *J Biomed Mater Res A* **89** 895-908

[14] Marelli B, Ghezzi C E, James-Bhasin M and Nazhat S N 2015 Fabrication of injectable, cellular, anisotropic collagen tissue equivalents with modular fibrillar densities *Biomaterials* **37** 183-93

[15] Kamranpour N O, Miri A K, James-Bhasin M and Nazhat S N 2016 A gel aspiration-ejection system for the controlled production and delivery of injectable dense collagen scaffolds *Biofabrication* **8** 015018

[16] Douglas J F 2018 Weak and Strong Gels and the Emergence of the Amorphous Solid State *Gels* **4**

[17] Gao T, Gillispie G J, Copus J S, Pr A K, Seol Y J, Atala A, Yoo J J and Lee S J 2018 Optimization of gelatin-alginate composite bioink printability using rheological parameters: a systematic approach *Biofabrication* **10** 034106

[18] O'Rourke C, Drake R A, Cameron G W, Jane Loughlin A and Phillips J B 2015 Optimising contraction and alignment of cellular collagen hydrogels to achieve reliable and consistent engineered anisotropic tissue *Journal of biomaterials applications* **30** 599-607

[19] Griffanti G, Rezabeigi E, Li J, Murshed M and Nazhat S N 2020 Rapid Biofabrication of Printable Dense Collagen Bioinks of Tunable Properties *Advanced Functional Materials* **30** 1903874

[20] Bilston L E, Liu Z and Phan-Thien N 1997 Linear viscoelastic properties of bovine brain tissue in shear *Biorheology* **34** 377-85

[21] Brands D W, Bovendeerd P H, Peters G W and Wismans J S 2000 The large shear strain dynamic behaviour of in-vitro porcine brain tissue and a silicone gel model material *Stapp Car Crash J* **44** 249-60

[22] Hrapko M, van Dommelen J A, Peters G W and Wismans J S 2006 The mechanical behaviour of brain tissue: large strain response and constitutive modelling *Biorheology* **43** 623-36
[23] Cheng S, Clarke E C and Bilston L E 2008 Rheological properties of the tissues of the central nervous system: a review *Med Eng Phys* **30** 1318-37
[24] Kocen R, Gasik M, Gantar A and Novak S 2017 Viscoelastic behaviour of hydrogel-based composites for tissue engineering under mechanical load *Biomed Mater* **12** 025004
[25] Kayal C, Shipley R J and Phillips J B 2019 Physical and mechanical properties of RAFT-stabilised collagen gels for tissue engineering applications *J Mech Behav Biomed Mater* **99** 216-24
[26] Barberio C G, Chaudhry T, Power D M, Tan S, Lawless B M, Espino D M and Wilton J C 2019 Towards viscoelastic characterisation of the human ulnar nerve: An early assessment using embalmed cadavers *Med Eng Phys* **64** 15-22
[27] Gildner C D, Lerner A L and Hocking D C 2004 Fibronectin matrix polymerization increases tensile strength of model tissue *American journal of physiology. Heart and circulatory physiology* **287** H46-53
[28] Roeder B A, Kokini K, Sturgis J E, Robinson J P and Voytik-Harbin S L 2002 Tensile mechanical properties of three-dimensional type I collagen extracellular matrices with varied microstructure *J Biomech Eng* **124** 214-22
[29] Seliktar D, Black R A, Vito R P and Nerem R M 2000 Dynamic mechanical conditioning of collagen-gel blood vessel constructs induces remodeling in vitro *Ann Biomed Eng* **28** 351-62
[30] Abou Neel E, Cheema U, Knowles J, Brown R and N. Nazhat S 2006 Use of multiple unconfined compression for control of collagen gel scaffold density and mechanical properties *Soft Matter* **2** 986-92
[31] Tsintou M, Dalamagkas K and Seifalian A 2018 Injectable Hydrogel versus Plastically Compressed Collagen Scaffold for Central Nervous System Applications *Int J Biomater* **2018** 3514019
[32] Zitnay J L, Reese S P, Tran G, Farhang N, Bowles R D and Weiss J A 2018 Fabrication of dense anisotropic collagen scaffolds using biaxial compression *Acta Biomater* **65** 76-87
[33] Borschel G H, Kia K F, Kuzon W M, Jr. and Dennis R G 2003 Mechanical properties of acellular peripheral nerve *J Surg Res* **114** 133-9
[34] Topp K S and Boyd B S 2006 Structure and biomechanics of peripheral nerves: nerve responses to physical stresses and implications for physical therapist practice *Phys Ther* **86** 92-109
[35] Georgeu G A, Walbeehm E T, Tillett R, Afoke A, Brown R A and Phillips J B 2005 Investigating the mechanical shear-plane between core and sheath elements of peripheral nerves *Cell Tissue Res* **320** 229-34
[36] Garvican E R, Cree S, Bull L, Smith R K and Dudhia J 2014 Viability of equine mesenchymal stem cells during transport and implantation *Stem Cell Res Ther* **5** 94
[37] Kim J, Andersson K E, Jackson J D, Lee S J, Atala A and Yoo J J 2014 Downregulation of metabolic activity increases cell survival under hypoxic conditions: potential applications for tissue engineering *Tissue engineering. Part A* **20** 2265-72
[38] Cheema U, Rong Z, Kirresh O, Macrobert A J, Vadgama P and Brown R A 2012 Oxygen diffusion through collagen scaffolds at defined densities: implications for cell survival in tissue models *J Tissue Eng Regen Med* **6** 77-84
[39] Amer M H, Rose F, Shakesheff K M, Modo M and White L J 2017 Translational considerations in injectable cell-based therapeutics for neurological applications: concepts, progress and challenges *NPJ Regen Med* **2** 23
[40] Jessen K R, Mirsky R and Lloyd A C 2015 Schwann Cells: Development and Role in Nerve Repair *Cold Spring Harb Perspect Biol* **7**
[41] Madison R D, Sofroniew M V and Robinson G A 2009 Schwann cell influence on motor neuron regeneration accuracy *Neuroscience* **163** 213-21
[42] Thompson D M and Buettner H M 2004 Oriented Schwann cell monolayers for directed neurite outgrowth *Ann Biomed Eng* **32** 1120-30

[43] Cheema U, Nazhat S N, Alp B, Foroughi F, Anandagoda N, Mudera V and Brown R A 2007 Fabricating tissues: Analysis of farming versus engineering strategies *Biotechnology and Bioprocess Engineering* **12** 9-14
[44] Wnek G E and Bowlin G L 2008 *Encyclopedia of biomaterials and biomedical engineering* (New York: Informa Healthcare USA)
[45] Zhou C, Liu B, Huang Y, Zeng X, You H, Li J and Zhang Y 2017 The effect of four types of artificial nerve graft structures on the repair of 10-mm rat sciatic nerve gap *J Biomed Mater Res A* **105** 3077-85
[46] Wang C Y, Zhang K H, Fan C Y, Mo X M, Ruan H J and Li F F 2011 Aligned natural-synthetic polyblend nanofibers for peripheral nerve regeneration *Acta Biomater* **7** 634-43
[47] Chang C J and Hsu S H 2006 The effect of high outflow permeability in asymmetric poly(dl-lactic acid-co-glycolic acid) conduits for peripheral nerve regeneration *Biomaterials* **27** 1035-42
[48] Kalbermatten D F, Pettersson J, Kingham P J, Pierer G, Wiberg M and Terenghi G 2009 New fibrin conduit for peripheral nerve repair *Journal of reconstructive microsurgery* **25** 27-33
[49] McGrath A M, Brohlin M, Kingham P J, Novikov L N, Wiberg M and Novikova L N 2012 Fibrin conduit supplemented with human mesenchymal stem cells and immunosuppressive treatment enhances regeneration after peripheral nerve injury *Neurosci Lett* **516** 171-6
[50] Yannas I V and Hill B J 2004 Selection of biomaterials for peripheral nerve regeneration using data from the nerve chamber model *Biomaterials* **25** 1593-600
[51] Schuh C, Day A G E, Redl H and Phillips J 2018 An Optimized Collagen-Fibrin Blend Engineered Neural Tissue Promotes Peripheral Nerve Repair *Tissue engineering. Part A* **24** 1332-40
[52] Muangsanit P, Shipley R J and Phillips J B 2018 Vascularization Strategies for Peripheral Nerve Tissue Engineering *Anatomical record* **301** 1657-67
[53] Bearden S E and Segal S S 2004 Microvessels promote motor nerve survival and regeneration through local VEGF release following ectopic reattachment *Microcirculation* **11** 633-44
[54] Chalfoun C, Scholz T, Cole M D, Steward E, Vanderkam V and Evans G R 2003 Primary nerve grafting: A study of revascularization *Microsurgery* **23** 60-5
[55] Best T J, Mackinnon S E, Midha R, Hunter D A and Evans P J 1999 Revascularization of peripheral nerve autografts and allografts *Plastic and reconstructive surgery* **104** 152-60
[56] O'Rourke C, Day A G E, Murray-Dunning C, Thanabalasundaram L, Cowan J, Stevanato L, Grace N, Cameron G, Drake R A L, Sinden J and Phillips J B 2018 An allogeneic 'off the shelf' therapeutic strategy for peripheral nerve tissue engineering using clinical grade human neural stem cells *Sci Rep* **8** 2951
[57] Suaid C, Santos A, Yamane F and Fazan V 2016 Aspects of the Macro and Microscopic Anatomy of the Sciatic Nerve in Wistar Rats *International Journal of Morphology* **34** 877-84
[58] Bell M A and Weddell A G 1984 A morphometric study of intrafascicular vessels of mammalian sciatic nerve *Muscle & nerve* **7** 524-34
[59] Haynes L W, Rushton J A, Perrins M F, Dyer J K, Jones R and Howell R 1994 Diploid and hyperdiploid rat Schwann cell strains displaying negative autoregulation of growth in vitro and myelin sheath-formation in vivo *J Neurosci Methods* **52** 119-27
[60] Tannemaat M R, Eggers R, Hendriks W T, de Ruiter G C, van Heerikhuize J J, Pool C W, Malessy M J, Boer G J and Verhaagen J 2008 Differential effects of lentiviral vector-mediated overexpression of nerve growth factor and glial cell line-derived neurotrophic factor on regenerating sensory and motor axons in the transected peripheral nerve *Eur J Neurosci* **28** 1467-79